U.P.B. Sci. Bull., Series D, Vol. 69, No. 1, 2007 ISSN 1454-2358

COMPARATIVE THREE DIMENSIONAL FRACTURE ANALYSES OF CRACKED PLATES

P.M.G.P. MOREIRA[1], Ş. D. PASTRAMĂ[2], P.M.S.T. de CASTRO[3]

În această lucrare, se prezintă soluţii tridimensionale pentru factorul de intensitate a tensiunii în placi cu fisuri centrale, utilizând metoda elementelor finite. Pentru comparaţie, pe lângă soluţiile din literatura de specialitate, in articol se obţin şi rezultate prin analize bidimensionale atât cu elemente finite cât şi cu metoda dual ă a elementelor de frontieră. Sunt prezentate concluzii referitoare la variaţia factorului de intensitate a tensiunii pe grosimea plăcii precum şi la acurateţea analizei tridimensionale, funcţie de discretizarea utilizată.

In this paper, three dimensional stress intensity factor solutions are obtained for a plate with a central crack using the Finite Element Method. For comparison of the 3D solutions, further to reference solutions given by the literature, two dimensional Finite Element analyses and 2D Dual Boundary Element Method analyses were performed. Conclusions are drawn regarding the variation of the Stress Intensity Factor along the thickness and the accuracy of the 3D analyses depending on the mesh refinement.

Keywords: finite element method, dual boundary element method, stress intensity factor

1. Introduction

In many structures, cracks may appear during manufacturing process or in service. Such cracks may grow in time, due to either static or fatigue loading, leading to the loss of strength in the structure. In order to avoid possible catastrophic failures, the behaviour of the crack must be known. For this, the knowledge of the crack size, service stress, material properties and stress intensity factor (SIF) are required. Many researchers have drawn their attention to the analytical, numerical or experimental methods of calculating the stress intensity factor. For complex configurations, numerical methods are used, as the finite element method (FEM) or the boundary element method (BEM). In the field of

[1] Doctoral Student, Department of Mechanical Engineering and Industrial Management, University of Porto, PORTUGAL
[2] Professor, Department of Strength of Materials, University "Politehnica" of Bucharest, RoMANIA
[3] Professor, Department of Mechanical Engineering and Industrial Management, University of Porto, PORTUGAL

numerical investigations of cracked structures, the two-dimensional (2D) analyses are usually adopted, since they are much simpler and less time consuming than the three dimensional (3D) ones, and with a reasonable degree of accuracy in most cases. However, the state of deformation near the crack tip is always 3D, as it was shown since the early work of Kassar and Sih [0]. That is why, especially in the last years that have brought an unprecedented development of computers, the 3D analysis of cracked structures has been used extensively, in order to produce more accurate numerical solutions for the stress and strain fields around the crack tip.

The plate-like structures having different types of cracks were analyzed by many researchers. The first analysis of a plate of finite thickness containing a through crack was made by Hartranft and Sih [0], [0] who obtained the stress distribution close to the crack front and made an attempt to determine the stress intensity factor distribution along the thickness. Further, other researchers have drawn their attention to this problem, with focus on the crack tip singularity and the stress behaviour in the boundary layers, at the intersection of the crack front with the free surface of the plate, see for example [0], [0], [0].

Three dimensional analyses of thin cracked plates were also presented by Nakamura and Parks [0] and Shivakumar and Raju [0], who performed refined 3D finite element analyses in order to obtain stress distributions and stress intensity factor values.

A recent detailed 3D analysis was presented by Kwon and Sun [0] who investigated the stress field near the crack tip, the degree of plane strain and the crack tip singularity. They suggested also a simple technique to determine 3D SIF at the plate mid-plane from a 2D analysis.

In this paper, refined 3D finite element analyses are performed in order to obtain the variation of the stress intensity factor along the thickness of a finite plate having a through-the-thickness central crack. Three different thickness values were used, in order to have both thin and thick plate behaviour.

The results were compared with values from the literature and also with results obtained using both the 2D FEM and the dual boundary element method (DBEM). The influence of the specimen geometry and mesh refinement on the SIF values and also and the drop of the SIF values at the intersection of the crack front with the free surface of the plate are discussed.

Conclusions are drawn regarding the accuracy of the 3D analysis and the necessity of using such a time-consuming analysis instead of a simpler 2D one.

2. Numerical techniques

Two numerical methods are used in this paper in order to determine SIF: the Finite Element Method and the Dual Boundary Element Method (DBEM). The *J* integral technique is used both in FEM and DBEM analyses to obtain SIF

solutions. In DBEM, results were also obtained using the singularity subtraction technique (SST) [0], [0]. A brief description of these techniques is given further.

2.1. The J-integral technique

The J integral is a contour integral, originally defined assuming non-linear elastic behaviour, introduced by Eshelby [0] and Rice [0]. The *J* integral is widely accepted as a fracture mechanics parameter for both linear and nonlinear material response. It is related to the energy release associated with crack growth and it is a measure of the intensity of deformation at a notch or crack tip, especially for nonlinear materials. If the material response is linear, the *J* integral can be related to the stress intensity factors. The finite element code ABAQUS [0] provides a procedure for evaluation of the *J* integral based on the virtual crack extension/domain integral methods. This parameter avoids the difficulties of the characterization of the stress field near the crack tip using local parameters such as the Crack Opening Displacement (COD), because its value is independent of the chosen contour Γ surrounding the crack tip (Fig. 1).

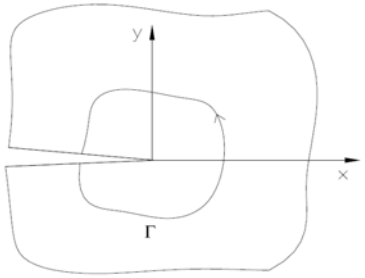

Fig. 1. Contour for the determination of J integral.

The analytical definition of *J* integral is given by the relationship:

$$J = \int_{\Gamma} w \cdot dy - \overline{T} \frac{\partial \overline{u}}{\partial x} \mathrm{d}s \,, \tag{1}$$

where w is the strain energy density in points of the contour, $\overline{T}$ is the traction vector, $\overline{u}$ is the displacement and ds the element of the contour Γ.

For calculation of the *J* integral in a 2D analysis using ABAQUS, the domain is described through rings of elements around the crack mouth. Different contours are created. The first contour consists of the elements linked directly to the nodes of the crack tip. The following contour consists of a ring of elements in contact with the first. Each subsequent contour is defined by the next ring of

elements. Even with coarse meshes it is possible to obtain precise values of J integral, [0].

The stress intensity factors K_I, K_{II} and K_{III} are used in linear elastic fracture mechanics to characterize the local crack-tip stress and displacement fields. They are related to the energy release rate (the J integral) through the equation:

$$J = \frac{1}{8\pi} K^T \cdot B^{-1} \cdot K \tag{2}$$

where $K = [K_I, K_{II}, K_{III}]^T$ are the SIFs and B is called the pre-logarithmic energy factor matrix. For homogeneous and isotropic materials, the above equation becomes simpler as follows:

$$J = \frac{1}{\bar{E}}\left(K_I^2 + K_{II}^2\right) + \frac{1}{2G} K_{III}^2 , \tag{3}$$

where $\bar{E} = E$ for plane stress and $\bar{E} = E/(1-\nu^2)$ for plane strain, axial symmetry, and three dimensions.

The SIF values obtained near the surface should be neglected due to difficulties of J integral calculation near a free surface [0]. A solution to this issue is to refine the mesh in this area. In the 3D analyses the SIF value obtained using only nodes in the outside surface of the plate were not taken into account.

For 3D SIF, results are presented in two different ways. In a first study, results for coordinates along the thickness are presented; each coordinate represents a layer of nodes. In the second study, using the three results of SIF for each element, and according to Fig. 2 and equation 4, an average value of SIF is calculated as:

$$K_{average} = \frac{K_A + 4K_B + K_C}{6} \tag{4}$$

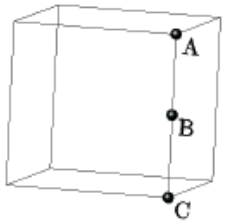

Fig. 2. Average stress intensity factor for an element.

When comparing a 3D analysis with a 2D one, attention should be given to the type of problem that is analysed: plane strain or plane stress. When a thin plate

is loaded parallel to the plane of the plate and the load is distributed uniformly over the thickness, the stress components σ_z, τ_{xz} and τ_{yz} are assumed to be zero, [0]. When the thickness of the body is very large, it is assumed that a plane strain state is present. In this case, γ_{yz}, γ_{zx} and ε_z are zero.

2.2. The Singularity Subtraction Technique

The SST technique associated with the Dual Boundary Element Method uses a particular solution of the BEM analysis, representing the singular field around the crack tip of a semi-infinite crack. Such a singular field is defined using the first term of the Williams series expansion.

One point in front of the crack tip is considered in this technique, implemented in DBEM in the post-processing phase [0]. The normal and shear stresses, denoted in Fig. 3 as $t_1 = \sigma$ and $t_2 = \tau$ respectively at an internal point at a distance ε as close as possible to the crack tip, are determined from the boundary element analysis.

The stress intensity factors K_I and K_{II} are obtained from the following equations:

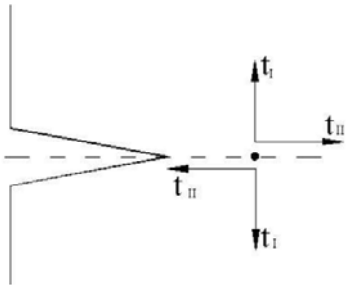

Fig. 3. Tractions at a point.

$$K_I = t_I \sqrt{2\pi r}$$
$$K_{II} = t_{II} \sqrt{2\pi r} \tag{5}$$

In equations (5), the stress σ is taken as σ_p (a numerical approximation of the stress at an internal point P placed at a distance ε ahead of the crack tip, Fig. 4). Also, one must use a value of the distance r for which that stress should exist. Notice that ε and r can have independent values, since they represent different approximations. The calibration of r was carried out taking into account several reference cases with known values of SIFs. In a previous work by Matos *et al.* [0], the values which give good results for a large variety of tested cases, were

adopted as $\varepsilon = 0,\ 0075\ l_e$ and $r = 0{,}0011\ l_e$, where l_e is the length of the boundary element closest to the crack tip.

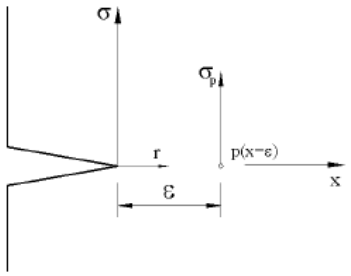

Fig. 4. Stress σ_p in a point P at a distance ε of the crack tip.

3. The studied structure

The structure considered for the present analysis is a center cracked finite plate, subjected to a remote uniform stress σ. Several geometric configurations for this study are defined according to Fig. 5. Note that the origin of the system of axes lies at the middle thickness plane.

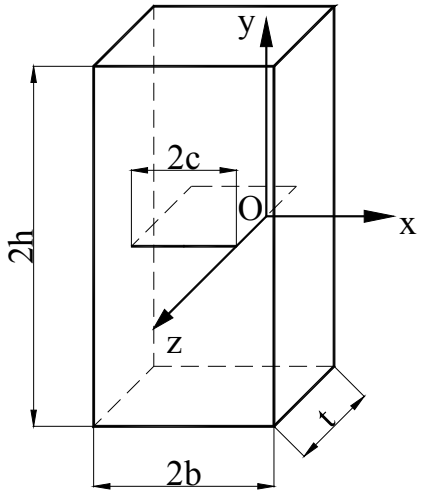

Fig. 5. Plate with a central crack.

The considered values of the ratios *h/b*, *c/b* and *t/c* are listed in Table 1, together with the reference solutions used for comparison.

Table 1

The studied geometries of the plate

h/b	c/b	*t/c*	Reference value
0.5	0.5	0.5	3D FEM; 2D FEM and DBEM; literature
		0.25	2D FEM and DBEM; literature
		1	

4. Results and discussions

According to Tada *et al* [0] the nondimensional 2D SIF $K/(\sigma\sqrt{\pi c})$ for the center cracked plate with h/b = 0.5 and c/b = 0.5 is 1.9145. First, 2D analyses were performed, using both FEM and DBEM. For the 2D DBEM analysis, SIFs were obtained using the J integral technique and the SST..

The finite element analysis was performed using 6840 eight noded plane CPE8 elements, while for the DBEM analysis the mesh contained only 60 elements (Fig. 6).

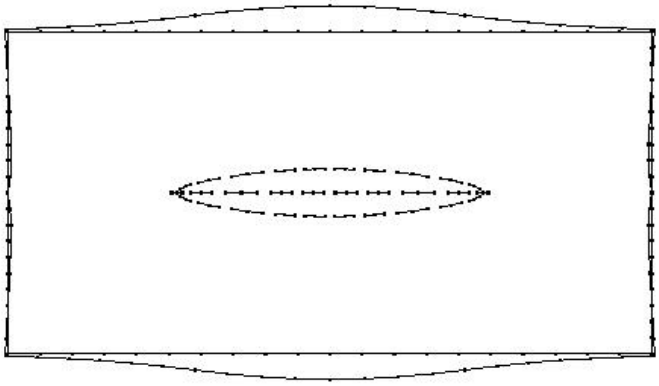

Fig. 6. Deformed and undeformed mesh for the 2D DBEM analysis

The results obtained with these techniques are listed in Table 2.

Table 2

2D results, FEM 2D and DBEM

Tada [0]	FEM 2D (J integral)		DBEM (J integral)		DBEM (SST)	
	Solution	Difference [%]	Solution	Diference [%]	Solution	Diference [%]
1.9145	1.9651	2.64	1.9884	3.86	1.9480	1.75

Then, a 3D FEM analysis was performed, for each of the three values of the ratio *t/c*, presenting the results in two different ways (nodal and element SIF), as mentioned in paragraph 1.1.

In order to calculate SIF for the 3D analysis, a mesh with 19440 elements and another one with 67200 elements were used in all cases. Only half of the plate was modelled. In the first mesh, 6 elements were placed along the thickness while in the second mesh 16 elements were used along the thickness. The plate was modelled with 20 nodes brick isoparametric elements (C3D20).

4.1. The case *t/c* = 0.5

In Fig. 7 is presented a detail of the less refined mesh showing the stress distribution in the load direction when a remote stress of 100 units is applied.

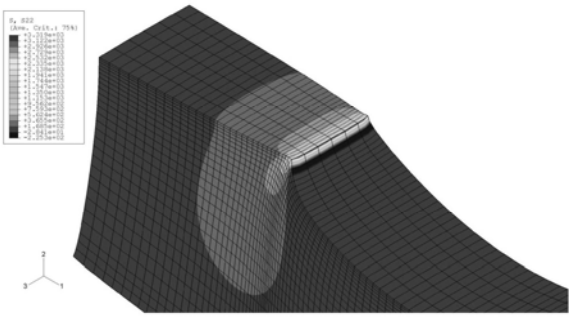

Fig. 7. Mesh detail for the 3D analysis: plot of the stress σ_y (19440 elements, *t/c* = 0.5).

Table 3 and Table 4 show the values of the nodal non-dimensional K along the thickness for the two different meshes used.

Studying the differences between the 3D FEM and the results from [0], one can see that in this case the use of a more refined mesh is useless; the errors are practically the same.

Fig. 8 shows the values of non-dimensional K along the thickness for the different meshes used, together with the reference 3D solutions found in Raju and Newman [0] and Atluri and Kathiresan [0] and the 2D results from this study.

Table 3

Non-dimensional 3D SIF along the thickness for the mesh with 19440 elements (*t/c* = 0.5)

Node layer	*z/t*	$K/(\sigma\sqrt{\pi c})$	Tada [0]	Difference [%]
1	0,5000	1,8297	1,9145	-4,4317
2	0,4167	2,0059		4,7751
3	0,3333	2,0613		7,6665
4	0,2500	2,0700		8,1230
5	0,1667	2,0817		8,7317
6	0,0833	2,0831		8,8078
7	0,0000	2,0846		8,8839

Table 4

Non-dimensional 3D FEM SIF along the thickness for the 67200 elements mesh (*t/c* = 0.5)

Node layer	*z/t*	$K/(\sigma\sqrt{\pi c})$	Tada [0]	Difference [%]
1	0,5000	1,7189		-10,2145
2	0,4688	1,9316		0,8945
3	0,4375	1,9986		4,3946
4	0,4063	2,0205		5,5360
5	0,3750	2,0423		6,6773
6	0,3438	2,0511		7,1339
7	0,3125	2,0613		7,6665
8	0,2813	2,0671		7,9708
10	0,2500	2,0729	1,9145	8,2752
11	0,2188	2,0758		8,4274
12	0,1875	2,0788		8,5795
13	0,1563	2,0802		8,6556
14	0,1250	2,0831		8,8078
15	0,0938	2,0831		8,8078
16	0,0625	2,0846		8,8839
17	0,0313	2,0846		8,8839
18	0,0000	2,0846		8,8839

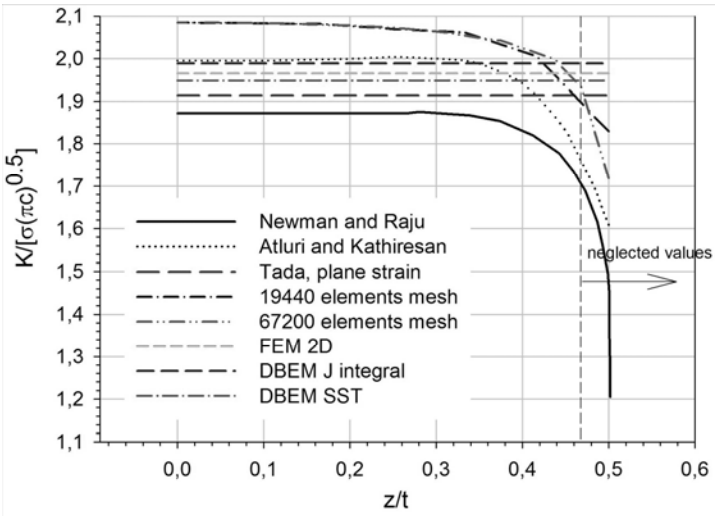

Fig. 8. Non-dimensional K along thickness (*t/c* = 0.5).

Table 5 presents values of the non-dimensional *K* in each element along the thickness at a crack tip for the 19440 elements mesh, calculated using equation (4). Layers 1 and 6 contain elements that lie on the surfaces; since the external nodes layer is averaged with the other two subsequent layers of nodes, the SIF

were not disregarded. SIFs obtained using the 3D FEM analyses are compared with Tada and DBEM SST results.

Table 5

3D FEM $K/(\sigma\sqrt{\pi c})$ for the 19440 elements mesh (t/c = 0.5)

Element layer	FEM 3D	Tada [0]		DBEM SST	
		Ref. value	Difference [%]	solution	Difference [%]
1	1,9858	1.9145	3,723	1.9884	-0,132
2	2,0705		8,148		4,129
3	2,0831		8,808		4,764
4	2,0831		8,808		4,764
5	2,0705		8,148		4,129
6	1,9858		3,723		-0,132

From the table above, it can be concluded that DBEM results show a good agreement with FEM 3D results.

4.2 The case t/c = 0.25

Table 6 and Table 7 show the values of non-dimensional K along the thickness for the different meshes used in this case.

Again, one can in this case the use of a more refined mesh is useless; the errors are practically the same.

Fig. 9 shows the values of non-dimensional K along the thickness for the different meshes used, DBEM J integral and SST analysis, and FEM 2D analysis.

Table 6

Non-dimensional 3D FEM SIF along thickness for the 19440 elements mesh (t/c = 0.25)

Node layer	z/t	$K/(\sigma\sqrt{\pi c})$	Tada [0]	Difference [%]
1	0,5000	1,8122	1.9145	-5,3448
2	0,4167	2,0074		4,8512
3	0,3333	2,0642		7,8187
4	0,2500	2,0744		8,3513
5	0,1667	2,0875		9,0361
6	0,0833	2,0890		9,1122
7	0,0000	2,0919		9,2644

Table 7

Non-dimensional 3D FEM SIF along thickness for the 67200 elements mesh (*t/c* = 0.25)

Node layer	*z/t*	$K/(\sigma\sqrt{\pi c})$	Tada [0]	Diference [%]
1	0,5	1,6884		-11,8124
2	0,468751	1,9316		0,8945
3	0,4375	1,9957		4,2425
4	0,406251	2,0219		5,6121
5	0,375	2,0453		6,8295
6	0,343751	2,0540		7,2860
7	0,3125	2,0642		7,8187
8	0,281251	2,0715		8,1991
10	0,25	2,0773	1.9145	8,5035
11	0,218751	2,0802		8,6556
12	0,1875	2,0846		8,8839
13	0,156251	2,0860		8,9600
14	0,125	2,0890		9,1122
15	0,093751	2,0904		9,1883
16	0,0625	2,0904		9,1883
17	0,031251	2,0919		9,2644
18	0	2,0919		9,2644

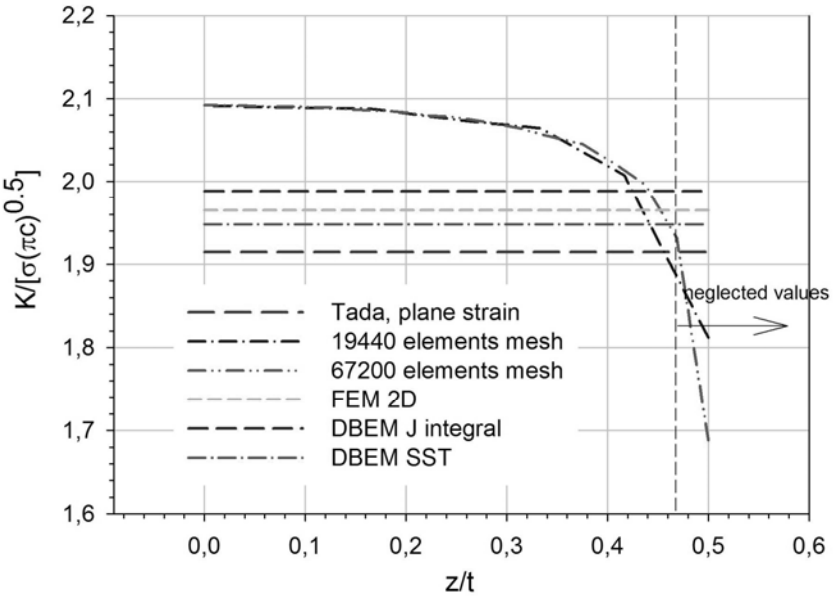

Fig. 9. Non-dimensional K along the thickness (*t/c* = 0.25).

Table 8 presents values of non-dimensional K in each element along the thickness at the crack tip for the mesh with 19440 elements. Again, DBEM results show a good agreement with FEM 3D results.

Table 8

3D FEM $K/(\sigma\sqrt{\pi c})$ for the 19440 elements mesh (t/c = 0.25)

Element layer	FEM 3D	Tada [0]		DBEM SST	
		ref value	Difference [%]	solution	Difference [%]
1	1,9843	1.9145	3,646	1.9884	-0,206
2	2,0749		8,377		4,349
3	2,0892		9,125		5,069
4	2,0892		9,125		5,069
5	2,0749		8,377		4,349
6	1,9843		3,646		-0,206

4.3 The case t/c = 1

In Table 9 and Table 10, the values of non-dimensional K along the thickness for the different meshes used are listed. Fig. 10 shows the values of non-dimensional K along the thickness for the different meshes used, DBEM J integral and SST analysis and FEM 2D analysis.

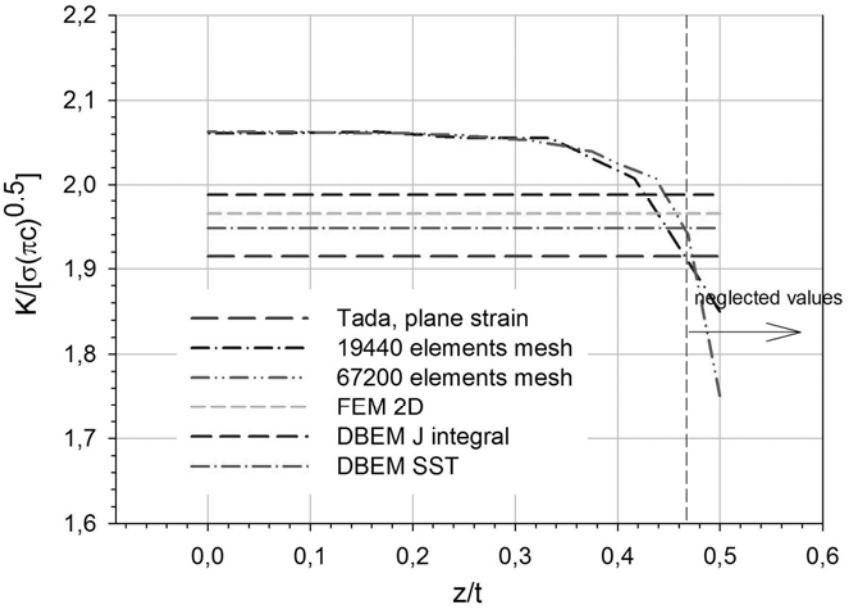

Fig. 10. Non-dimensional K along the thickness (t/c = 1).

Table 9

Non-dimensional 3D FEM SIF along thickness for the 19440 elements mesh (*t/c* = 1)

Node layer	z/t	$K/(\sigma\sqrt{\pi c})$	Tada [0]	Difference [%]
1	0,5000	1,8500		-3,3665
2	0,4167	2,0074		4,8512
3	0,3333	2,0554		7,3621
4	0,2500	2,0554	1.9145	7,3621
5	0,1667	2,0627		7,7426
6	0,0833	2,0613		7,6665
7	0,0000	2,0613		7,6665

Table 10

Non-dimensional 3D FEM SIF along thickness for the 67200 elements mesh (*t/c* = 1)

Node layer	z/t	$K/(\sigma\sqrt{\pi c})$	Tada [0]	Diference [%]
1	0,5	1,7510		-8,5406
2	0,468751	1,9404		1,3511
3	0,4375	2,0074		4,8512
4	0,406251	2,0219		5,6121
5	0,375	2,0394		6,5251
6	0,343751	2,0467		6,9056
7	0,3125	2,0525		7,2099
8	0,281251	2,0554		7,3621
10	0,25	2,0584	1.9145	7,5143
11	0,218751	2,0598		7,5904
12	0,1875	2,0613		7,6665
13	0,156251	2,0613		7,6665
14	0,125	2,0613		7,6665
15	0,093751	2,0627		7,7426
16	0,0625	2,0627		7,7426
17	0,031251	2,0627		7,7426
18	0	2,0627		7,7426

Table 11 presents values of non-dimensional K in each element along the thickness at a crack tip for the 19440 elements mesh.

In this case also, DBEM results show a good agreement with FEM 3D results.

4.4 Comparison of results

A comparison between the 3D SIF results obtained for the several plate thickness and the 2D reference results is presented in Fig. 11. From this figure, a similar trend followed by the 3D SIF can be noticed both in this analysis and in

the 3D reference values from the literature: the stress intensity factor has a slow variation at the middle of the plate but decreases dramatically near the free surface.

Table 11

3D FEM $K/(\sigma\sqrt{\pi c})$ for the 19440 elements mesh ($t/c = 1$)

Element layer	FEM 3D	Tada [0]		DBEM SST	
		ref value	Diference [%]	solution	Diference [%]
1	1,9892	1.9145	3,90	1.9884	0,04
2	2,0567		7,43		3,43
3	2,0615		7,68		3,68
4	2,0615		7,68		3,68
5	2,0567		7,43		3,43
6	1,9892		3,90		0,04

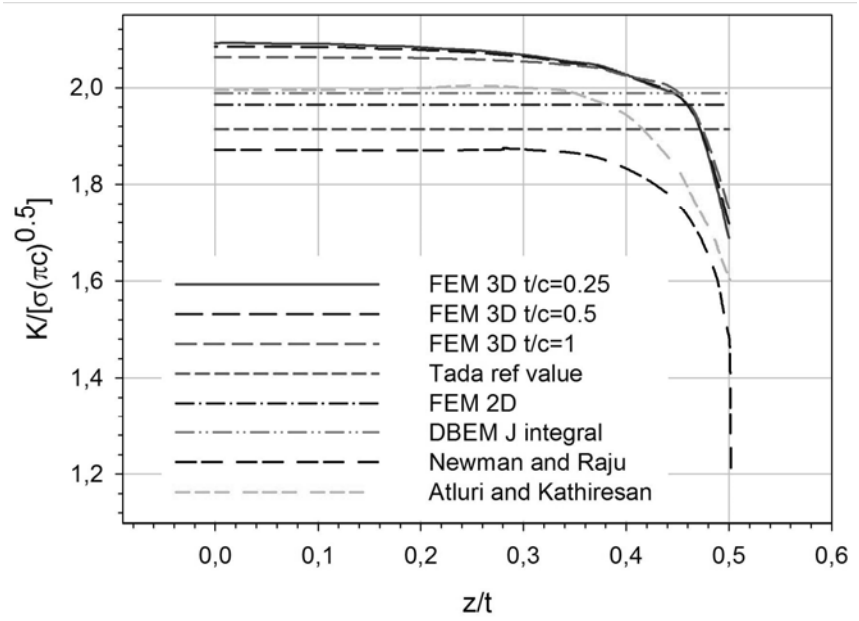

Fig. 11. Non-dimensional K for each studied plate thickness.

5. Conclusions

In this paper, FEM and DBEM analyses were used in order to obtain SIF solutions for a cracked finite plate, with the *J* integral and Singularity Subtraction techniques. To convert the *J* integral into SIF values in a 2D analysis, the expressions $J = K_I^2/E$ for plane stress and $J = K_I^2 \cdot (1 - \nu^2)/E$ for plane strain are used. Nevertheless, it should be noticed that the *J* solution is not the same in a plane stress and plane strain analysis. So, at the end it results the SIF for a plane

stress analysis is equal to the SIF for a plane strain analysis. In a 2D numerical simulation, despite carrying out a plane strain analysis or a plane stress analysis, leading to different strain and stress results, K_I solutions are independent of the type of analysis.

In a 3D analysis, SIF has different values through the thickness. So, a 2D SIF analysis is only an approximation of the exact solution since there is no difference on plane stress or plane strain SIF solutions for LEFM.

Values of SIF obtained in Raju and Newman [0] and Atluri and Kathiresan [0] are lower than those obtained in the 3D FEM analyses. A parametric study was carried out in order to assess the influence of mesh refinement in the final solution. It was found that a good agreement between the present 3D analysis and the solution in [0] is obtained even when using coarse meshes. Nevertheless it should be reminded that the 3D references solutions were obtained with FEM meshes created in the middle 70's when computational resources were quite low.

When comparing reference SIF solutions (literature or 2D FEM or DBEM) with 3D FEM SIFs, the best agreement was found when using the SIF value in the external layer of elements.

R E F E R E N C E S

[1] *M.K. Kassir, G.C. Sih*, "Three dimensional stress distribution around an elliptical crack under arbitrary loadings", in Transactions of ASME, Journal of Applied Mechanics, **vol. 33**, 1966, pp. 601-611.

[2] *R.J. Hartranft, G.C. Sih*, "The use of eigenfunction expansions in the general solution of three dimensional crack problems", in Journal of Mathematics and Mechanics, **vol. 19**, 1969, pp. 123-138.

[4] *R.J. Hartranft, G.C. Sih*, "An approximate three dimensional theory of plates with application to crack problems', in International Journal of Engineering Science, **vol. 8**, 1970, pp. 711-729.

[5] *J.P. Benthem*, "State of stress at the vertex of a quarter infinite crack in the half space", in International Journal of Solids and Structures, **vol. 13**, 1977, pp. 479-492.

[6] *A.F. Bloom*, *B. Andersson*, "On the semi-elliptical surface crack problem: Detailed numerical solutions for complete elastic stress fields", in Surface-Crack Growth: Models, Experiments and Structures, ASTM STP 1060 (W.G. Reuter et al., Eds.), Philadelphia, American Society for Testing and Materials, 1990, pp. 77-98.

[7] *W.X. Zhu*, "Singular stress fields of three diemnsional crack", in Engineering Fracture Mechanics, **vol. 36**, 1990, pp. 239-244.

[8] *T. Nakamura, D.M. Parks*, "Three dimensional stress field near the crack front of a thin elastic plate", in Journal of Applied Mechanics, **vol. 55**, 1988, pp. 805-813.

[9] *K.N. Shivakumar*, *I.S. Raju*, "Treatment of singularities in cracked bodies, in International Journal of Fracture, **vol. 45**, 1990, pp. 159-178.

[10] *S.W. Kwon*, *C.T. Sun*, "Characteristics of three dimensional stress fields in plates with through-the-thickness crack", in International Journal of Fracture, **vol. 104**, 2000, pp. 291-315.

[11] *A. Portela*, "Dual Boundary Element analysis of crack growth", in Computational Mechanics Publications Southampton UK and Boston USA. 1993.

[12] *P.F.P. de Matos, P.M.G.P. Moreira, A. Portela, P.M.S.T. de Castro,* "Dual Boundary Element Analysis of Cracked Plates: Post-Processing Implementation of the Singularity Subtraction Technique", in Computers & Structures. **vol. 82**, nr. 17-19, 2004, pp. 1443-1449.

[13] *J. D. Eshelby*, "The continuum theory of lattice defects", in Solid State Physics, **vol.** 3, 1956, pp. 79-141.

[14] *J. R. Rice*, "Mathematical analysis in the mechanics of fracture", in Fracture. an Advanced Treatise", **vol.** II, New York, 1968, pp. 191-308.

[15] * * * ABAQUS, Fracture mechanics (course notes), Karlson Hibbitt and Sorensen Inc. 1991.

[16] *S. P. Timoshenko*, *J. N. Goodier*, Theory of Elasticity, International Student edition. 3rd edition. McGraw-Hill, New York, 1970.

[17] *H. Tada, P.C. Paris, G.R. Irwin*, "The stress analysis of cracks handbook", ASME Press, New York, 2000.

[18] *I.S. Raju, J.C. Newman Jr.,* "Three dimensional finite-element analysis of finite-thickness fracture specimens", NASA Center for AeroSpace Information (CASI) NASA-TN-D-8414; L-10967. 19770501, May 1, 1977.

[19] *S. Atluri, K. Kathiresan*, "An Assumed Displacement Hybrid Finite Element Model for Three-Dimensional Linear-Fracture-Mechanics Analysis", in Proceedings of the 12th Annual Meeting of the Society of Engineering Science, 1975, pp. 391-399.